Cancer Management and Research

Dovepress

open access to scientific and medical research

Open Access Full Text Article

ORIGINAL RESEARCH

# CBX3 Promotes Gastric Cancer Progression and Affects Factors Related to Immunotherapeutic Responses

This article was published in the following Dove Press journal:
*Cancer Management and Research*



Hexin Lin[1,2,*]
Jiabian Lian[3,4,*]
Lu Xia[4,5,*]
Guoxian Guan[2]
Jun You[1,4]

[1]Department of Gastrointestinal Surgery, The First Affiliated Hospital of Xiamen University, Xiamen, People's Republic of China; [2]Department of Colorectal Surgery, The First Affiliated Hospital of Fujian Medical University, Fuzhou, People's Republic of China; [3]Department of Laboratory Medicine, Xiamen Key Laboratory of Genetic Testing, The First Affiliated Hospital of Xiamen University, Xiamen, People's Republic of China; [4]School of Clinical Medicine, Fujian Medical University, Fuzhou, People's Republic of China; [5]Laboratory of Cancer Center, The First Affiliated Hospital of Xiamen University, Xiamen, People's Republic of China

*These authors contributed equally to this work

**Background:** Chromobox 3 (CBX3) is a member of the chromobox family proteins, which plays a critical role in tumor progression, but the exact function of CBX3 in gastric cancer remains unknown. The current research mainly investigates the underlying mechanisms and clinical value of CBX3 in gastric cancer.

**Methods:** Gene expression cohorts from The Cancer Genome Atlas (TCGA) and Gene Expression Omnibus (GEO) were analyzed to assess the effect of CBX3 in gastric cancer. CBX3 expression was further determined by immunohistochemistry (IHC). The function of CBX3 on proliferation, migration and the cell cycle was explored via colony-forming, cell cycle and transwell assays, respectively. Moreover, RNA sequencing (RNA-seq) in AGS cells and two cohorts was utilized to explore the specific mechanism of CBX3.

**Results:** CBX3 expression was upregulated in human gastric cancer tissues and the expression level was closely associated with adverse signs. Knockdown of CBX3 in gastric cancer cells significantly inhibited the malignant phenotype. In addition, RNA-seq analysis revealed that CBX3 regulates genes related to the cell cycle, mismatch repair and immune-related pathways. Furthermore, the expression of CBX3 was significantly and inversely related to the abundance of tumor-infiltrating lymphocytes (TILs), PDCD1 and PDCD1LG2 expression and immunotherapy responses. Moreover, CBX3 influences the effectiveness of chemotherapy, thereby impacting the prognosis of gastric cancer patients.

**Conclusion:** CBX3 contributes to gastric cancer progression and is associated with chemotherapy and immunotherapy response. CBX3 may serve as a new diagnostic biomarker and potential target for immunotherapy and chemotherapy in gastric cancer.

**Keywords:** chromobox 3, gastric cancer, tumorigenesis, survival, chemotherapy, immunotherapy

## Introduction

Gastric cancer (GC) has become the fifth most prevalent and the third most deadly carcinoma due to its high malignancy.[1] Although surgical resection is the radical treatment for GC, many patients with advanced disease are not eligible for curative surgical treatment and develop recurrence and metastasis. Therefore, it is urgent to explore the potential pathogenic mechanism and provide new strategies for GC therapy.

Heterochromatin protein 1 (HP1) is a major component of heterochromatin and consists of three orthologs: CBX1, CBX3 and CBX5. CBX3 can recognize and bind to histone H3 lysine 9 (H3K9) to recruit many functional cofactors,[2,3] with

Correspondence: Jun You
Department of Gastrointestinal Surgery, The First Affiliated Hospital of Xiamen University, Teaching Hospital of Fujian Medical University, 55 Zhenhai Road, Xiamen, Fujian 361000, People's Republic of China
Tel +86-13906051681
Email junyou_fahxm@163.com

submit your manuscript | www.dovepress.com
DovePress
http://doi.org/10.2147/CMAR.S271807

cellular functions that include the DNA damage response,[4,5] transcriptional regulation,[6] telomere function[7] and cell differentiation.[8] CBX3 is widely overexpressed in several types of tumors, including colorectal cancer, breast cancer, hepatocellular carcinoma, tongue cancer and lung carcinoma. However, the function of CBX3 in GC has not yet been verified. Therefore, we designed this study to elucidate the function of CBX3 in GC as well as its molecular mechanism.

# Methods

## Genomic Data Sources

Transcriptome sequencing data and somatic mutation data for 375 GC patients were downloaded from the TCGA data portal (portal.gdc.cancer.gov/) as the cohort TCGA-STAD. Clinicopathological data for TCGA-STAD cohort were downloaded from Xena (xena.ucsc.edu/). A total of 209 stomach tissue transcriptome sequencing data as a normal group were downloaded from the GTEx portal (www.gtexportal.org). Multiple GC datasets (GSE14210, GSE15459, GSE22377, GSE 29,272, GSE51105) containing transcriptome sequencing and the clinicopathological datasets for 638 GC patients were downloaded from GEO (www.ncbi.nlm.nih.gov/geo/). The GEO-GC cohort was used for verification. The tissue transcriptome sequencing dataset GSE2669 and the single-cell transcriptome sequencing dataset GSE134520 were used to analyze genetic changes from gastritis to GC. Single-cell gene expression data were normalized, scaled and clustered using the R package "Seurat", see previous research for detailed methods.[9] Multiple PD-1 immunotherapy transcriptome sequencing datasets (GSE13157, GSE79691, GSE67501, GSE99070) were downloaded from Gene Expression Omnibus. Batch effects were corrected using the "ComBat" algorithm of the R package "sva". Patients were divided into a high CBX3 expression group and a low CBX3 expression group based on quartile values.

## Mutational Analysis

The TISIDB database integrates the relationships between expression of CBX3 and immune subtypes and molecular subtypes in GC (cis.hku.hk/TISIDB/index.php).[10] The R package "maftools" was applied to analyze genes frequently mutated in the cohort TCGA-STAD. The patients in this cohort were also divided into a high CBX3 expression group and a low CBX3 expression group based on CBX3 mRNA expression quartile values. The TMB of each TCGA-STAD cohort patient was calculated according to the number of nonsynonymous somatic cell variations per megabase as previously described.[11] The tumor neoantigens were calculated by NetMHCpan,[12] and high-affinity peptides were defined as all possible 9–10mer mutant peptides with a rank score ≤0.5% and strong binding, as previously described.[13]

## Cell Culture

Human GC cells (AGS, NCI-N87) and HEK293T cells were purchased from the Chinese Academy of Sciences (CAS). NCI-N87 cells were cultured in RPMI 1640 (Gibco) with 10% fetal bovine serum (FBS), 1% Glutamax and 1% sodium pyruvate (100μm). AGS cells were cultured in F12K (Gibco) with 1% Sodium hydrogen carbonate and 10% FBS. HEK 293T cells were cultured in DMEM (Gibco) supplemented with 10% FBS. All cells were incubated in a humidified environment containing 5% carbon dioxide.

## Immunohistochemistry (IHC)

IHC was performed on tissue microarrays of GC (Outdo Biotech Co., Shanghai) following a previous study.[14] We used anti-CBX3 (Abcam) as the primary antibody. Immunoreactivity was determined by a semiquantitative method according to the staining intensity of cancer cells and the positively stained proportion. The scoring criteria for proportion of positively-staining tumor cells were as follows: 0, none; 1, 10%; 2, 11–50%; 3, 51–80%; and 4, >80%. The scoring criteria for the staining intensity: 0, no staining; 1, weak; 2, moderate; and 3, strong. We obtained the semiquantitative immune score by multiplying the positive cell score by the staining intensity score ranging from 0 to 12. This study was approved by the Ethical Review Board of the First Affiliated Hospital of Xiamen University.

## Plasmid Construction and Transfection

Two pairs of shRNA oligonucleotides targeting CBX3 were designed and cloned into the Eco RI/Age I sites in the pLKO.1-puro lentiviral vector. The recombinant plasmid was cotransfected together with pMD2.G/psPAX2 into HEK293T cells. pLKO.1-scramble shRNA was used as the control. Lentiviral particles were harvested from HEK293T and infected AGS and NCI-N87 cells followed by hygromycin screening. The shRNA sequences used in our study were as follows: sh-CBX3-1 F:5′-

CCGGCGACGTGTAGTGAATGGGAAACTCGAGTTT-CCCATTCACTACACGTCGTTTTTG-3′ and R: 5′-AA TTCAAAAACGACGTGTAGTGAATGGGAAACTCGA-GTTTCCCATTCACTACACGTCG-3′; sh-CBX3-2 F: 5′-CCGGGCGTTTCTTAACTCTCAGAAACTCGAGTT TCTGAGAGTTAAGAAACGCTTTTTG-3′ and R: 5′-AATTCAAAAAGCGTTTCTTAACTCTCAGAAACTC-GAGTTTCTGAGAGTTAAGAAACGC-3′.

## Western Blotting

All proteins were separated by SDS-PAGE, transferred to polyvinylidene difluoride membranes, and blocked with 3% bovine serum albumin (BSA) for 2 hours at room temperature. Primary antibodies (Abcam) were diluted with 3% BSA, applied at a 1:1000 dilution to the membranes and incubated at 4°C overnight, the appropriate secondary antibodies (Cell Signaling Technology) were incubated for 1 hour at room temperature. Protein expression was detected using the enhanced chemiluminescent HRP substrate (Cell Signaling Technology) and imaged with a Chemiluminescence Imaging System (Bio-Rad Laboratories).

## Real-Time Quantitative

RT-PCR was performed using a Reverse Transcriptase M-MLV kit (Takara) in accordance with the manufacturer's protocol, and a LightCycler 480 RT-PCR system (Roche) with Power SYBR Green PCR Master Mix (Takara). Expression of CBX3 was calculated by the Ct value, which was determined by comparison with β-actin. All experiments were repeated in triplicate, and the values obtained were averaged. The primers used in our study were as follows: forward primer: 5′-gagatgctgctgacaaacca -3′, reverse primer: 5′-accaagtctgcctcatctga-3′.

## Colony Forming Assay

Cells (200) were seeded in 6-well plates, fixed 14 days later with 3.7% paraformaldehyde for 5 min, and stained with 0.1% crystal violet for 15 min.

## Transwell Assay

Transwell chambers were placed into 24-well plates. The cell density was adjusted to $1\times10^5$ cells/mL, and 200μL of cell suspension in serum-free medium was added to the upper well. About 600μL of medium containing 10% FBS was added to the lower chamber and incubated at 37°C for 48 h. The cells on the lower surface of the membrane were washed twice with PBS, and the remaining cells on the upper surface of the membrane were wiped off with a wet cotton swab. The cells were immobilized with 4% paraformaldehyde for 30 min, stained with 0.5% crystal violet for 15 min, photographed and counted under a microscope.

## Cell Cycle Assay

Cells were harvested by trypsin and washed two times with PBS, fixed at −20°C in 75% ethanol for 12 hours and stained in 0.5 mL propidium iodide using a cell cycle analysis kit (Beyotime) following the manufacturer's protocols. The cell cycle distribution was assessed by flow cytometry (BD FACS Canto II). The results were analyzed using Flowjo 7.6 software.

## RNA Sequencing (RNA-Seq) Analysis

Total RNA was extracted from AGS cells stably transfected with PLKO.1-puro-sh-CBX3 or sh-scramble. RNA-seq was carried out using the Illumina HiSeq X Ten platform. RNA sequences were mapped to the human genome GRCh37/hg19 using STAR.[15] Differentially expressed genes (DEGs) were identified by edgeR based on the logFC > 0.5 and $P$-value < 0.05. To interpret the biological functions of the DEGs, Gene Ontology (GO) was performed using DAVID v6.8 (david.ncifcrf.gov/home.jsp).[16] Gene set enrichment analysis (GSEA) of the cohorts TCGA-STAD and GEO-GC were divided into high and low CBX3 expression groups and analyzed using GSEA Desktop v3.0 software.

## Analysis of Immunotherapy Influencing Factors and Immunotherapy Response

TIMER was used to explore the influence of CBX3 expression in each tumor-infiltrating immune cell in GC (B cell, CD4+ T cells, CD8+ T cells, neutrophils, macrophages, and dendritic cells) (timer.cistrome.org/).[17] The tumor mutational burden (TMB) and neoantigen were analyzed with TCGA-STAD profile data. Spearman analysis was employed to evaluate the relationship of CBX3 with immune checkpoint genes. Multiple GEO datasets (GSE13157, GSE79691, GSE67501, GSE99070) for different cancers were applied to estimate the role of CBX3 in anti-PD-1 therapy. ImmunCellAI was utilized to predict the response to immune checkpoint blockade (ICB) therapy using the cohorts TCGA-STAD and GEO-GC (bioinfo.life.hust.edu.cn/web/ImmuCellAI/).[18]

## Chemotherapeutic Survival Analysis and Response Prediction

Overall survival (OS) analysis was performed for 344 patients who were followed-up for more than 30 days in the cohort TCGA-STAD. The R package "TCGAbiolinks" was applied to download chemotherapeutic information. The chemotherapeutic response prediction used the R package "pRRophetic" to estimate the half-maximal inhibitory concentration (IC50) of each STAD patient on the Genomics of Drug Sensitivity in Cancer (GDSC) website, with tissues type set to "digestive system" and the dataset parameter set to "cqp2016". Survival differences for patients treated with 5-fluorouracil (5-FU)-based chemotherapy were validated in the GSE14210 dataset.

## Statistical Analysis

Student's *t*-test and one-way ANOVA were used for intergroup comparisons of continuous variables. All continuous variables are presented as the mean ± SEM. The Chi-square test and Fisher's exact test were employed for comparisons of quantitative variables. Spearman correlation tests were applied to compare the correlation between sample factors. Survival analysis involved Log rank tests and Kaplan–Meier curves. $P$-values $< 0.05$ were considered statistically significant. The statistical analysis was performed using SPSS 23.0.

# Results

## CBX3 is Upregulated in Human Gastric Cancer Tissues

The difference in mRNA expression of CBX3 in GC and normal tissues was investigated in the cohort TCGA-STAD. CBX3 expression was higher in human GC tissues than in paired normal tissue and GTEx normal stomach tissue (Figure 1A and B). According to ROC curve analysis, CBX3 was a good predictor of GC (Figure 1C and D). Additionally, the expression level of CBX3 increased continuously from chronic gastritis to intestinal metaplasia, and to early GC (Figure 1E). CBX3 expression in stem cells was significantly higher than that of other cells in single-cell sequencing data, and CBX3 expression was significantly increased from precancerous lesions to early gastric cancer (Figure 1F, Figure S1). Immunohistochemistry of GC tissues and paracancerous tissues showed that CBX3 protein expression was significantly elevated in tumor tissues (Figure 1G and H).

## Correlation of CBX3 Expression with Clinicopathological Parameters

Based on the cohort TCGA-STAD cohort, we analyzed the correlation of CBX3 expression with clinicopathological characteristics in gastric cancer. The high expression of CBX3 is closely related to the T stages (Figure 1I). There was no difference in the expression of CBX3 between different pathologic N stages and M stages (Table S1). The mRNA expression level of CBX3 in patients with antrum or distal gastric carcinoma was markedly higher than that in patients with gastroesophageal junction carcinoma (Figure 1J), and CBX3 expression was significantly higher in MSI-H GC patients than the level of MSS patients (Figure 1K). Moreover, CBX3 expression was associated with the number of positive lymph nodes (Figure 1L).

## CBX3 Indicates High-Frequency Somatic Mutation

As somatic mutations have been shown to be involved in the development of cancer, we analyzed somatic mutation in GC using TCGA-STAD to investigate the difference in somatic mutation between high and low CBX3 groups. We observed significant differences in CBX3 expression in different molecular subtypes of GC, whereby CBX3 expression was lower in genome-stable subtype than in the other subtypes (Figure 2A). In addition, the average number of variants in the CBX3 high group was greater than that in the CBX3 low group (Figure 2B and C). Common mutations were shown in the waterfall plot and stratified by CBX3 expression level (Figure 2D and E). Somatic mutation profiles revealed that the tumor suppressor gene TP53 was more frequently mutated in the high CBX3 expression group (Figure 2F).

## CBX3 Promotes the Progression of Human Gastric Cancer Cells

To investigate the correlation between CBX3 and malignant phenotype of GC, CBX3 expression was reduced in NCI-N87 and AGS cells by using shRNA constructs. The expression levels of CBX3 mRNA and protein in both cell lines of the CBX3 shRNA group (sh-CBX3) were markedly lower than those in the control group (sh-NC) (Figure 3A and B). Furthermore, cloning formation assays demonstrated that silencing CBX3 expression inhibited the proliferation capacity of GC cells (Figure 3C), and transwell assays indicated reduced invasion ability in GC cells when

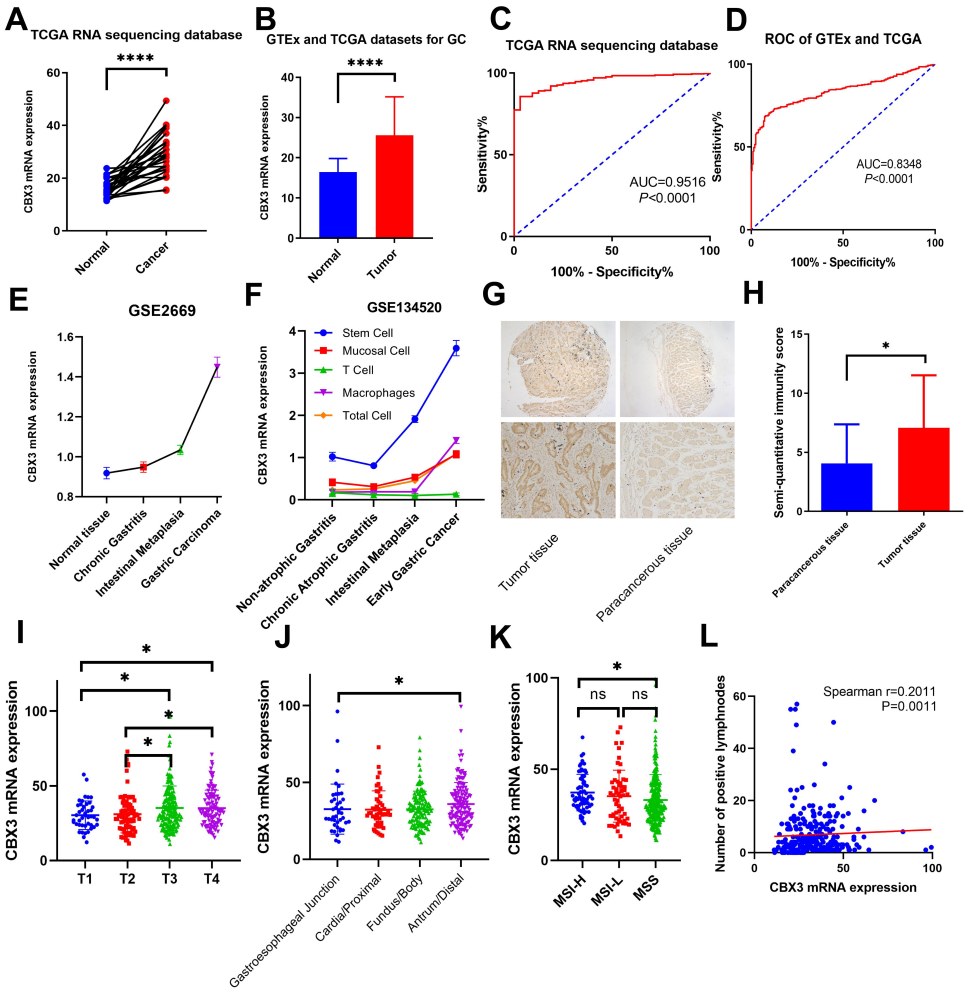


**Figure 1** The relationship between CBX3 expression and clinicopathological data. (**A** and **B**) Differential expression of CBX3 in normal stomach and gastric cancer tissues. (**C** and **D**) Evaluation of the sensitivity and specificity of gastric cancer diagnosis by ROC curves. (**E**) Expression of CBX3 in normal gastric tissues, precancerous lesions and gastric cancer tissues in the GSE26690 dataset. (**F**) Changes of CBX3 expression in various cells in single-cell sequencing GSE134520 dataset. (**G**) Immunohistochemical staining for CBX3 in gastric cancer tissues (n=30). (**H**) Semiquantitative immunity score in gastric cancer tissues and paracancerous tissues. (**I**–**L**) The association of CBX3 expression levels with T stage, tumor location, microsatellite instability and positive lymph nodes in the cohort TCGA-STAD. P value designations: ns: P≥ 0.05, *P < 0.05, ****P < 0.0001.

CBX3 was knocked down (Figure 3D). Therefore, we assessed cell cycle transition in the CBX3-knockdown GC cell line AGS and found that knocking down CBX3 resulted in cell cycle arrest at G1 phase (Figure 3E).

## CBX3 Promotes Tumor Progression via Multiple Signaling Pathways

To explore the molecular mechanism by which CBX3 directly promotes the malignant GC type, TCGA-STAD and GEO-GC cohorts were used for GSEA, and the results confirmed that CBX3-regulated genes to be associated with the cell cycle, DNA replication, mismatch repair and nucleotide metabolism-related pathways (Figure 4A and B). We further performed RNA-seq to investigate transcription level alterations after CBX3 silencing. The results show that the level of multiple genes was impacted by CBX3 expression, with 52 genes being upregulated and 81 genes downregulated in AGS cells. According to enrichment analysis of DEGs in the AGS cell line, CBX3 regulates a subset of genes highly enriched in the cell cycle, cell proliferation and interferon (IFN) signaling pathway (Figure 4C and D, Table S2). Further analysis of TCGA cohort and AGS RNA-seq showed that CBX3 expression was significantly correlated with genes related to cell cycle transition and DNA replication (Figure S2).

## Regulation of Immune Molecules by CBX3

As previously mentioned, CBX3 represses genes significantly related to the IFN signaling pathway and IFNs are critical cytokines that regulate both innate and adaptive

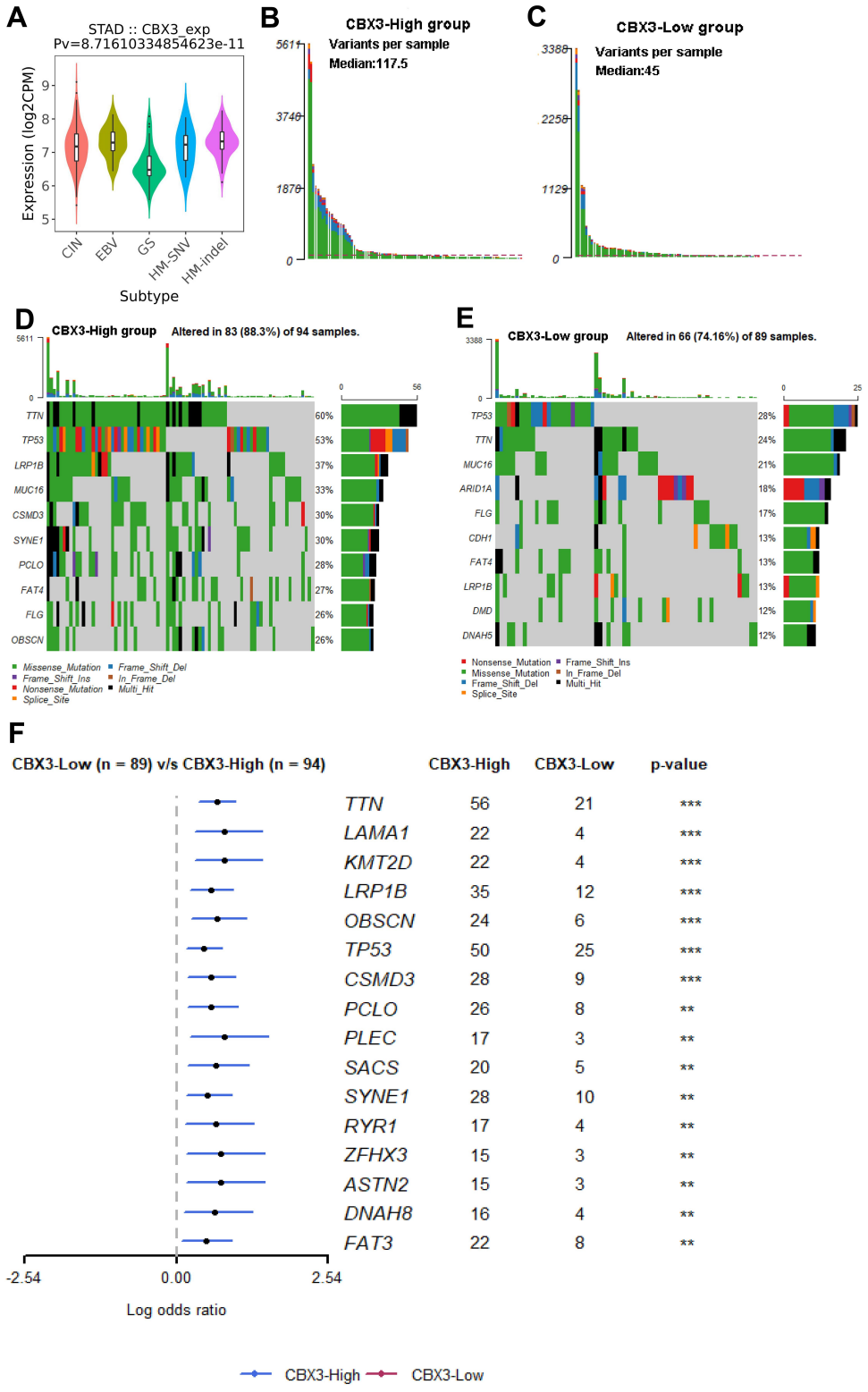


**Figure 2** Association between CBX3 and mutation alterations in the cohort TCGA-STAD (**A**) Distribution of CBX3 expression across molecular subtypes. (**B** and **C**) The average number of variants in the high and low CBX3 groups. (**D** and **E**) Common mutation information illustrated in the somatic mutation spectrum. (**F**) Significantly differentially expressed mutant genes in the high and low CBX3 groups. P value designations: **P < 0.01, ***P < 0.001.

**Abbreviations**: CIN, chromosomal instability; EBV, Epstein–Barr virus; GS, genome stable; HM-SNV, hypermutated single nucleotide variants; HM-Indel, hypermutated insertion deletion.

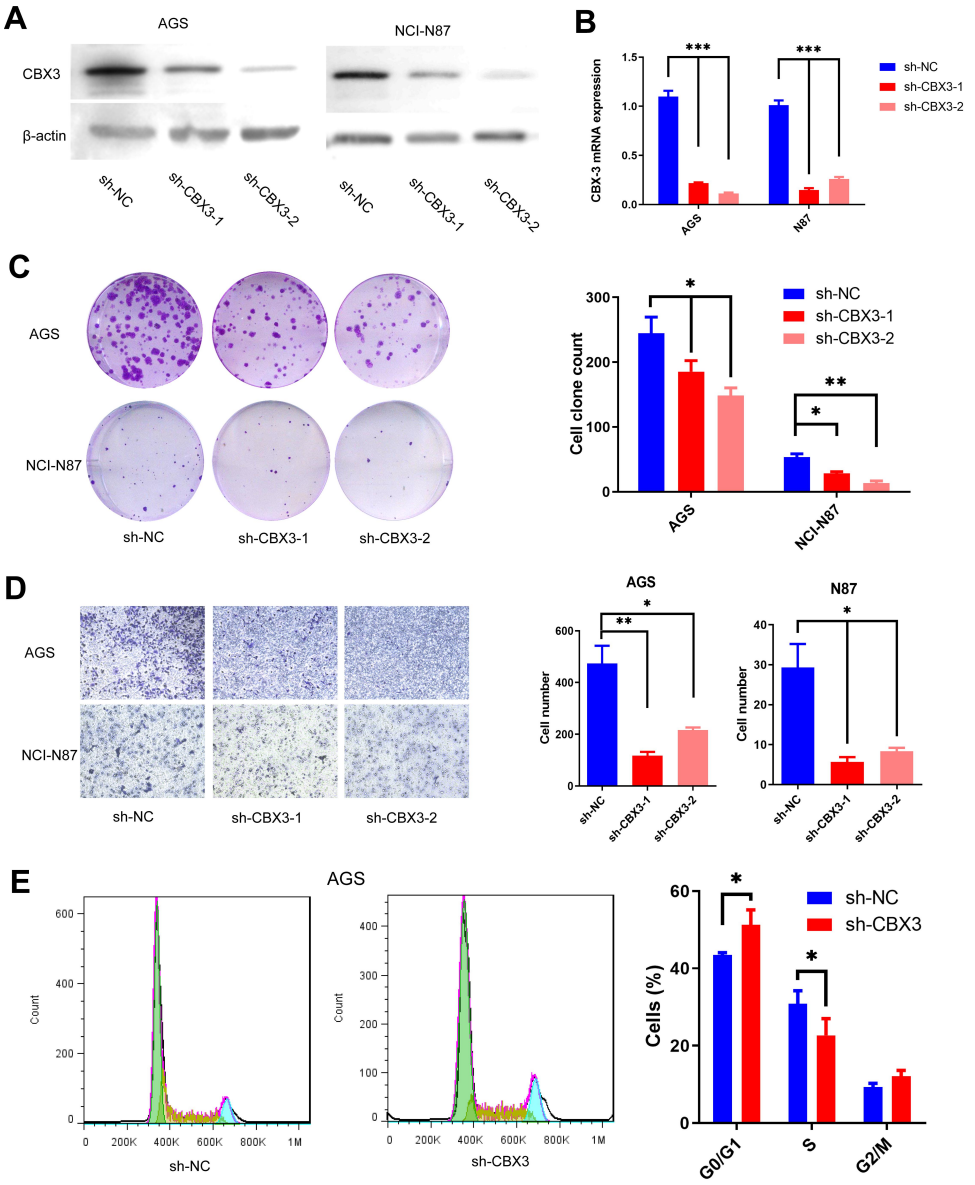


**Figure 3** CBX3 promoted GC cell progression. (**A**) CBX3 protein expression was detected following CBX3 knockdown in AGS and NCI-N87 cells. (**B**) CBX3 mRNA expression was detected following CBX3 knockdown in AGS and NCI-N87 cells. (**C**) GC cell proliferation was detected by cloning formation assays in the CBX3 knockdown group compared with the control group. (**D**) Transwell assays were performed to detect the effect of CBX3 knockdown on GC cell migration. (**E**) Flow cytometry assays were performed to analyze the cell cycle in sh-CBX3 GC cells. Values at different stages of the cell cycle. P value designations: *P < 0.05, **P < 0.01, ***P<0.001.

immunity. Previous studies have confirmed that both IFN-γ and type I interferon have roles in anticancer immunity and immunotherapeutic effects, and we analyzed the potential biological roles of CBX3 in tumor immunity. In GC, the abundance of B cells, CD8+ cells, CD4+ cells, macrophages, neutrophils and dendritic cells correlated negatively with CBX3 expression (Figure 5A). Next, we found that the neoantigen count and TMB correlated significantly and positively with CBX3 expression (Figure 5B). CBX3 expression was also closely related to immune checkpoint genes, including PDCD1, PDCD1LG2, CD274 and CTLA4 (Figure 5C), and the proportion of MSI-H in the CBX3 high expression group (22.9%) was significantly increased compared with that in the low expression group (12.4%) (Figure 5D).

Because CBX3 affects the immune microenvironment, TMB, microsatellite instability and other factors related to the efficacy of immunotherapy, we further investigated the relationship between the response to immune checkpoint blockade (ICB) therapy response and CBX3 expression.

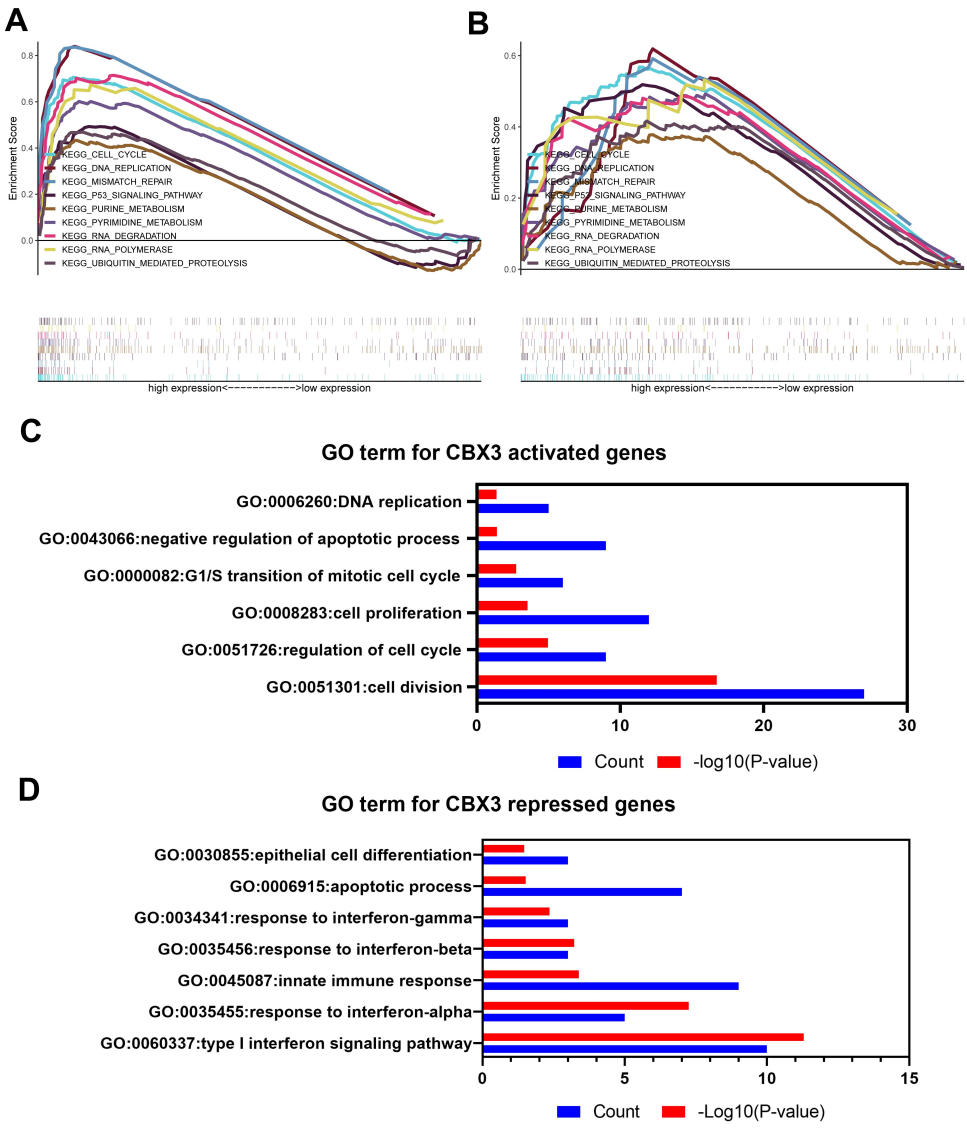


**Figure 4** (**A** and **B**) GSEA analysis of samples in the high and low CBX3 groups in the cohorts TCGA-STAD and GEO-GC. (**C** and **D**) GO analysis of differentially expressed genes in CBX3-knockdown AGS cells versus the control group.

Additionally, we analyzed data for patients of the four anti-PD-1 immunotherapy GEO datasets who exhibited high expression of CBX3 and a significant therapeutic response to anti-PD-1 immunotherapy (Figure 5E). Moreover, we predicted the immunotherapy response in the cohorts TCGA-STAD and GEO-GC cohort by ImmuCellAI, and the results showed that CBX3 expression in responder group was significantly less than that in nonresponder group (Figure 5F and G).

## CBX3 Contributes to the Sensitively of Gastric Cancer to Chemotherapy

To investigate the relationship between CBX3 expression and chemotherapy response, survival analysis was performed to examine survival differences between patients treated with and without chemotherapy. Although CBX3 can promote the malignant phenotype of GC cells, there was no survival advantage in the low CBX3 expression group (Figure 6A–C). In contrast, a survival advantage for the high CBX3 group compared with the low CBX3 group was observed in those who underwent chemotherapy, especially stage III patients (Figure 6D–F). However, in patients not treated with chemotherapy, there was a significant survival benefit in the low CBX3 group compared with the high CBX3 group (Figure 6G–I). We also predicted the sensitive to chemotherapies in high and low CBX3 groups by evaluating RNA-seq data of the cohorts TCGA-STAD and GEO-GC and observed that the estimated IC50 for 5-fluorouracil (5-FU) chemotherapy

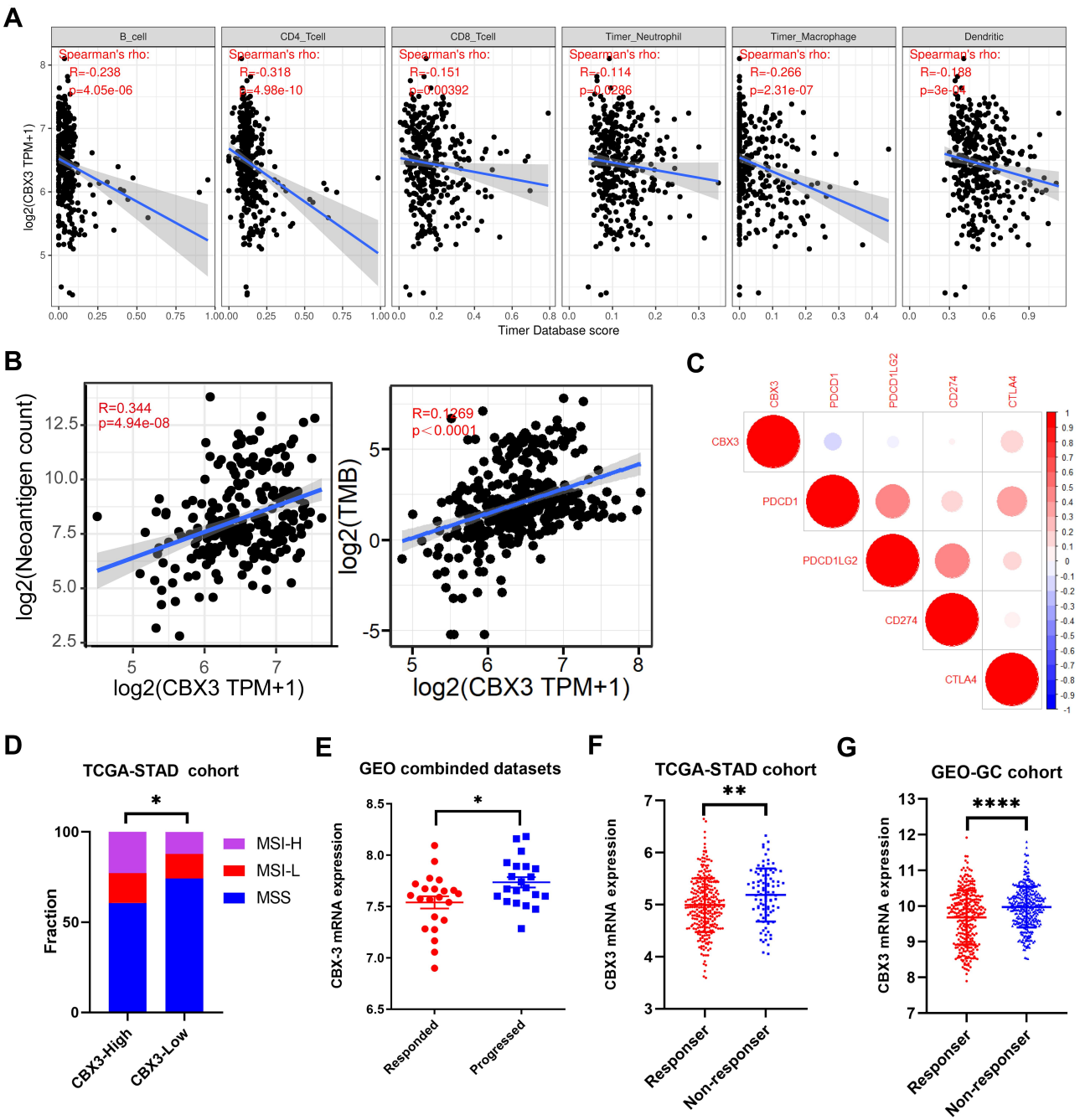


**Figure 5** Immunotherapeutic response related-factor analysis in the cohort TCGA. (**A**) Spearman correlation of CBX3 with the abundance of TILs in gastric cancer (TIMER). (**B**) Relationships between CBX3 expression and neoantigen and TMB. (**C**) Spearman correlation between PDCD1, PDCD1LG2, CD274, CTLA4 and CBX3 expression in gastric cancer. (**D**) Distribution of MSI status in high and low CBX3 groups. (**E**) The expression difference of CBX3 between the anti-PD-1 immunotherapy response and progression groups in the GEO combine dataset (n=43). (**F** and **G**) Differences in CBX3 expression between the immune checkpoint blockade response and nonresponse groups in TCGA-STAD and GEO-GC cohorts. P value designations: *P < 0.05, **P < 0.01, ****P<0.0001.
**Abbreviations**: TILs, tumor-infiltrating lymphocytes; TMB, tumor mutational burden; MSI, microsatellite instability.

was significantly different between the two groups, with high CBX3 expression increasing sensitivity to 5-FU chemotherapy (Figure 7A–D). Furthermore, among patients treated with 5-FU, the high CBX3 group lived longer than the low CBX3 group (Figure 7E and F).

## Discussion

To date, eight members of the CBX family have been identified in the human genome. The CBX family can be divided into the HP1 group and the Polycomb group according to molecular structure. The structure of HP1

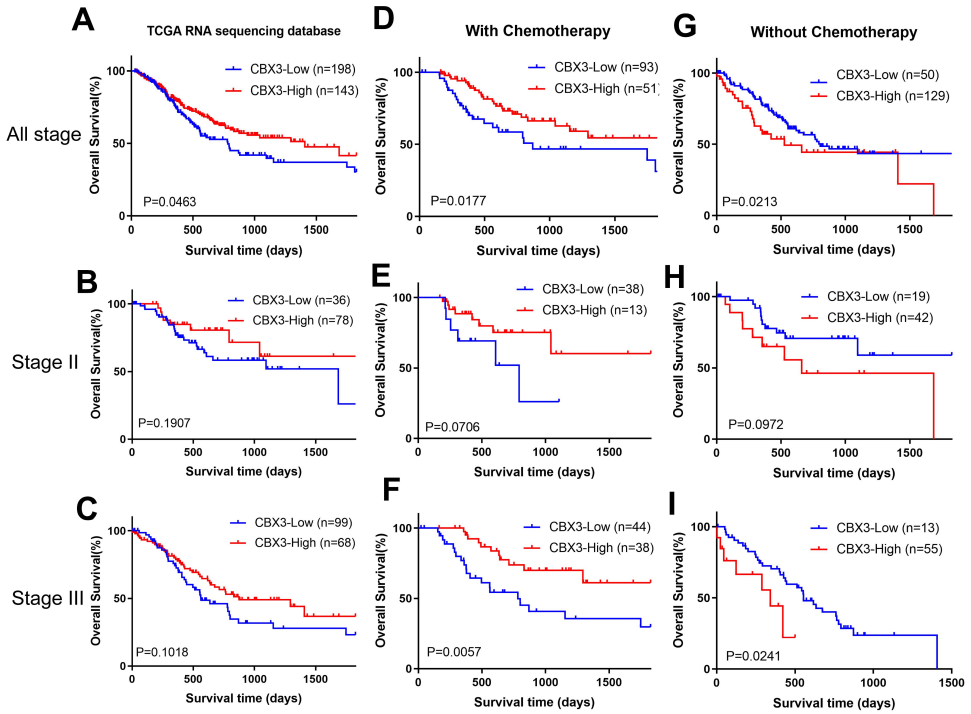


**Figure 6** Overall survival analysis stratified by chemotherapy and TNM stage in the cohort TCGA-STAD. (**A**–**C**) Survival curve of 5-year OS in all stage, stage II and stage III patients. (**D**–**F**) Survival curve of 5-year OS in the chemotherapy group. (**G**–**I**) Survival curve of 5-year OS in the without chemotherapy group.

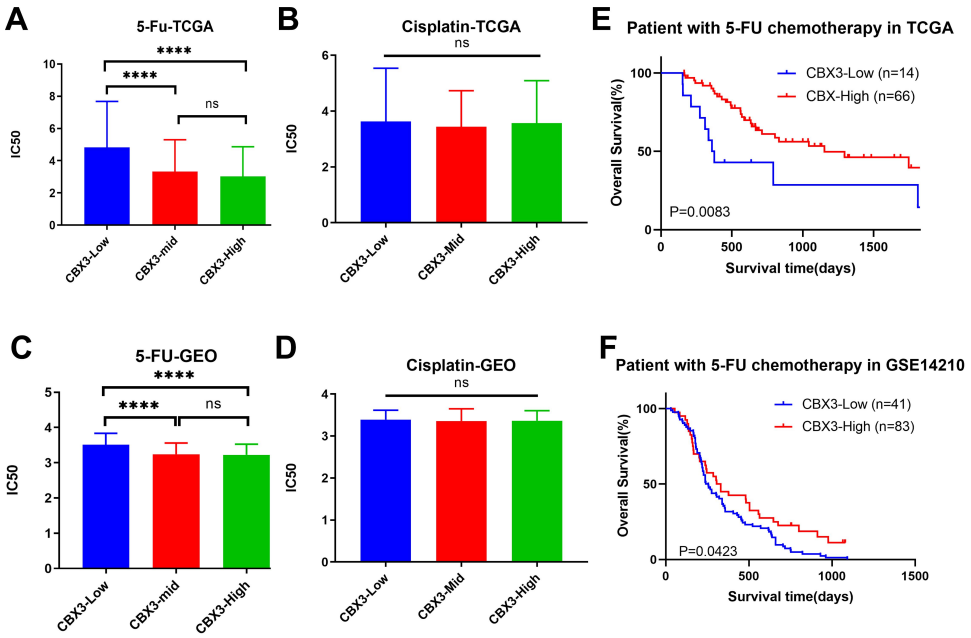


**Figure 7** CBX3 decreased chemotherapy resistance of gastric cancer in cohort TCGA-STAD and GEO-GC cohorts. Prediction of 5-fluorouracil (5-FU) (**A** and **C**) and cisplatin (**B** and **D**) in the high, medium and low CBX3 expression groups. Kaplan–Meier curves for overall survival in TCGA-STAD cohort and GSE14210 patients treated with 5-FU-based chemotherapy (**E** and **F**). P value designations: ns: P≥ 0.05, ****P < 0.0001.

consists of two characteristically conserved regions, an N-terminal chromodomain (CD) and a C-terminal chromo shadow domain (CSD), connected by a relatively unconserved hinge region.[19,20] The CD domain of the HP1 protein specifically recognizes h3k9 me2/3, dimer hydrophobic surface is formed between CSD domains to recruit specific proteins, and the hinge domain bind to nucleic acids.[21,22] CBX3-encoded HP1γ is a paralog of HP1,

which is widely known to be associated with euchromatin.[23,24] CBX3 participates in several molecular processes, including silencing of gene expression,[25,26] DNA damage repair,[4,27] and centromere cohesion protection.[28,29]

Previous studies have reported that aberrant expression of CBX3 is closely related to the prognosis of various cancers. Further experiments also confirm that CBX3 inhibition suppresses the progression of various cancer cell lines. However, there are few related studies in the field of GC to date. In our study, the proliferation and migration of the GC cell lines AGS and NCI-N87 were significantly reduced by inhibition of CBX3. Additionally, most of the existing studies emphasize the cell cycle regulation mediated by CBX3. For example, overexpression of CBX3 can modulate cell proliferation ability by promoting G1/S cell cycle transformation in tongue cancer,[30] osteosarcoma[31] and colon cancer.[32] Knocking down CBX3 can arrest cell cycle in the G2/M cell cycle transition, thereby suppressing the proliferation of cancer cells in pancreatic adenocarcinoma[33] and glioblastoma.[34] Similarly, our results show that CBX3 inhibition affects cell cycle transformation not only in G1/S phase but also in G2/M phase.

Radical surgery and adjuvant chemotherapy are the main treatments for advanced GC. As early as 2009, Takanashi et al found that CBX3 might serve as a therapeutic target for a variety of tumors.[35] In our research, patients with high expression of CBX3 had a better prognosis in the chemotherapy group, which was contrary to that in the non-chemotherapy group. These results indicate that CBX3 is a potential chemotherapy target and therapeutic efficacy predictor.

Immune checkpoint blockade using monoclonal antibodies has shown a long-lasting clinical response in GC,[36] and previous studies have confirmed that both IFN-γ and type I interferon participate in anticancer immunity and immunotherapeutic effect.[37] The results of our RNA-seq enrichment analysis showed enrichment of IFN-γ- and IFN-α/β-related pathways after CBX3 knockdown. Sun et al suggested that Cbx3/HP1γ deficiency can enhance the antitumor function of CD8+ effector T cells by increasing Prf1, Gzmb and IFN-γ expression in solid tumors.[38] PD-1 inhibitors have already become the most popular immunotherapy method. The response rate depends on programmed cell death protein 1 ligands (PDCD1LG) expression, besides, it is also influenced by MSI status, TILs and TMB.[39–44] Previous research has confirmed that TIL status can be a predictive biomarker for the prognosis of GC.[45] In our research, although a higher proportion of MSI, patients with high CBX3 expression had a higher proportion of MSI, as well as TMB and neoantigen, was observed for patients with high CBX3 expression, expression of CBX3 correlated significantly and negatively correlated with PDCD1 and PDCD1LG2 expression and TILs. In four studies, the CBX3 expression level of the anti-PD-1 responder group was significantly lower than that of the nonresponder group. Therefore, we hypothesized that CBX3 can inhibit the efficacy of PD-1 inhibitors by reducing TILs and expression of immune-related genes in GC tissues.

Several studies have shown that CBX3 participates in the maintenance of genomic stability and DNA damage repair.[4,5,46] In the analysis of GC subtypes, a high expression level of CBX3 was found in chromosomal-instability and high-mutation subtypes, but a low expression level in genome-stable subtypes. This result was further confirmed using TCGA-STAD somatic mutation data, and consistent results were obtained.

Chronic atrophic gastritis and intestinal metaplasia require rigorous examination as precancerous lesions. Bilgic et al reported that CBX3 was overexpressed in GC and atrophic gastritis (AG) groups compared with normal tissues, with the fold change levels of CBX3 in the GC group being well above those in the AG group.[47] According to our research, during the dynamic process from chronic inflammation to tumorigenesis, the expression level of CBX3 showed an increasing tendency in stomach biopsies. At the same time, through the analysis of a single-cell network constructed by Shao Li et al,[9] we found that CBX3 expression in stem cells was higher than that in other cells and increased significantly with the progression of premalignant lesions. The transition from chronic inflammation to cancer is a complex and lengthy process that involves multiple-scale changes in DNA damage responses, gene mutations, cell cycle regulation, inflammation and immune responses.[48] In this study, CBX3 was observed to influences the levels of the above factors and may be considered a promising marker for GC screening in populations at high-risk population of GC.

There are some limitations in this study. The exact mechanisms of CBX3-regulated TIL infiltration require further in vivo and in vitro experiments to confirm. Data on the anti-PD-1 response were obtained from public databases for several cancer types, and further immunotherapy

data for GC need to be collected to verify the role of CBX3. Despite these limitations, the results of this study provide a new potential target for predicting immunotherapy effects in GC. Hence, CBX3 may be a predictor of the efficacy of PD-1 inhibitors and a potential target of immunotherapy.

In conclusion, expression of CBX3 was upregulated in GC tissues. Furthermore, CBX3 correlated significantly with the malignant phenotype and down-regulated CBX3 significantly inhibited the tumorigenesis of GC cells. With further exploration, CBX3 expression was correlated with the efficacy-related factors of immunotherapy. This is the first study to demonstrate that CBX3 promotes tumor progression and influences pharmacotherapy response. These findings provide a new perspective for the GC progression and pharmacotherapy.

## Funding

This work was funded by the National Natural Science Foundation of China (Nos. 81802268), Fujian Provincial Department of Science and Technology (Nos. 2018J01381), Fujian Provincial Health Commssion (Nos.2018-2-60) and the Xiamen Municipal Health Commssion (Nos 3502Z20184022).

## Disclosure

The authors report no conflicts of interest for this work. Hexin Lin, Jiabian Lian and Lu Xia: first author; these authors contributed equally to this paper.

## References

1. Freddie B, Ferlay J, Soerjomataram I, et al. Global cancer statistics 2018: GLOBOCAN estimates of incidence and mortality worldwide for 36 cancers in 185 countries. *CA Cancer J Clin*. 2018;68(6):394–424.
2. Bannister Andrew J, Zegerman P, Partridge JF, et al. Selective recognition of methylated lysine 9 on histone H3 by the HP1 chromo domain. *Nature*. 2001;410(6824):120–124. doi:10.1038/35065138
3. Cheutin T, McNairn AJ, Jenuwein T, et al. Maintenance of stable heterochromatin domains by dynamic HP1 binding. *Science*. 2003;299(5607):721–725. doi:10.1126/science.1078572
4. Akaike Y, Kuwano Y, Nishida K, et al. Homeodomain-interacting protein kinase 2 regulates DNA damage response through interacting with heterochromatin protein 1gamma. *Oncogene*. 2015;34(26):3463–3473. doi:10.1038/onc.2014.278
5. Oka Y, Suzuki K, Yamauchi M, et al. Recruitment of the cohesin loading factor NIPBL to DNA double-strand breaks depends on MDC1, RNF168 and HP1γ in human cells. *Biochem Biophys Res Commun*. 2011;411(4):762–767. doi:10.1016/j.bbrc.2011.07.021
6. Rea S, Eisenhaber F, O'Carroll D, et al. Regulation of chromatin structure by site-specific histone H3 methyltransferases. *Nature*. 2000;406(6796):593–599. doi:10.1038/35020506
7. Canudas S, Houghtaling BR, Bhanot M, et al. A role for heterochromatin protein 1gamma at human telomeres. *Genes Dev*. 2011;25(17):1807–1819. doi:10.1101/gad.17325211
8. Caillier M, Thenot S, Tribollet V, et al. Role of the epigenetic regulator HP1gamma in the control of embryonic stem cell properties. *PLoS One*. 2010;5(11):e15507. doi:10.1371/journal.pone.0015507
9. Zhang P, Yang M, Zhang Y, et al. Dissecting the single-cell transcriptome network underlying gastric premalignant lesions and early gastric cancer. *Cell Rep*. 2019;27(6):1934–47 e5. doi:10.1016/j.celrep.2019.04.052
10. Ru B, Wong CN, Tong Y, et al. TISIDB: an integrated repository portal for tumor-immune system interactions. *Bioinformatics*. 2019;35(20):4200–4202. doi:10.1093/bioinformatics/btz210
11. Chalmers ZR, Connelly CF, Fabrizio D, et al. Analysis of 100,000 human cancer genomes reveals the landscape of tumor mutational burden. *Genome Med*. 2017;9(1):34. doi:10.1186/s13073-017-0424-2
12. Nielsen M, Lundegaard C, Blicher T, et al. NetMHCpan, a method for quantitative predictions of peptide binding to any HLA-A and -B locus protein of known sequence. *PLoS One*. 2007;2(8):e796. doi:10.1371/journal.pone.0000796
13. Hendrickx W, Simeone I, Anjum S, et al. Identification of genetic determinants of breast cancer immune phenotypes by integrative genome-scale analysis. *Oncoimmunology*. 2017;6(2):e1253654. doi:10.1080/2162402X.2016.1253654
14. Ye F, Chen Y, Xia L, et al. Aldolase A overexpression is associated with poor prognosis and promotes tumor progression by the epithelial-mesenchymal transition in colon cancer. *Biochem Biophys Res Commun*. 2018;497(2):639–645.
15. Dobin A, Davis CA, Schlesinger F, et al. STAR: ultrafast universal RNA-seq aligner. *Bioinformatics*. 2013;29(1):15–21. doi:10.1093/bioinformatics/bts635
16. Huang da W, Sherman BT, Lempicki RA. Systematic and integrative analysis of large gene lists using DAVID bioinformatics resources. *Nat Protoc*. 2009;4(1):44–57. doi:10.1038/nprot.2008.211
17. Li T, Fan J, Wang B, et al. TIMER: a web server for comprehensive analysis of tumor-infiltrating immune cells. *Cancer Res*. 2017;77(21):e108–e10. doi:10.1158/0008-5472.CAN-17-0307
18. Miao YR, Zhang Q, Lei Q, et al. ImmuCellAI: a unique method for comprehensive T-cell subsets abundance prediction and its application in cancer immunotherapy. *Adv Sci*. 2020;7(7):1902880.
19. Paro R, Hogness DS. The polycomb protein shares a homologous domain with a heterochromatin-associated protein of drosophila. *Proc Natl Acad Sci U S A*. 1991;88(1):263–267. doi:10.1073/pnas.88.1.263
20. Aasland R, Stewart AF. The chromo shadow domain, a second chromo domain in heterochromatin-binding protein 1, HP1. *Nucleic Acids Res*. 1995;23(16):3168–3173. doi:10.1093/nar/23.16.3168
21. Cowieson NP, Partridge JF, Allshire RC, et al. Dimerisation of a chromo shadow domain and distinctions from the chromodomain as revealed by structural analysis. *Curr Biol*. 2000;10(9):517–525. doi:10.1016/S0960-9822(00)00467-X
22. Meehan RR, Kao CF, Pennings S. HP1 binding to native chromatin in vitro is determined by the hinge region and not by the chromodomain. *EMBO J*. 2003;22(12):3164–3174. doi:10.1093/emboj/cdg306
23. Jones DO, Cowell IG, Singh PB. Mammalian chromodomain proteins: their role in genome organisation and expression. *BioEssays*. 2000;22(2):124–137. doi:10.1002/(SICI)1521-1878(200002)22:2<124::AID-BIES4>3.0.CO;2-E
24. Ogawa H, Ishiguro K, Gaubatz S, et al. A complex with chromatin modifiers that occupies E2F- and Myc-responsive genes in G0 cells. *Science*. 2002;296(5570):1132–1136. doi:10.1126/science.1069861
25. Canzio D, Larson A, Narlikar GJ. Mechanisms of functional promiscuity by HP1 proteins. *Trends Cell Biol*. 2014;24(6):377–386. doi:10.1016/j.tcb.2014.01.002
26. Smallwood A, Hon GC, Jin F, et al. CBX3 regulates efficient RNA processing genome-wide. *Genome Res*. 2012;22(8):1426–1436. doi:10.1101/gr.124818.111

27. Ball Alexander R, Yokomori K. Revisiting the role of heterochromatin protein 1 in DNA repair. *J Cell Biol*. 2009;185(4):573–575. doi:10.1083/jcb.200904033
28. Yi Q, Chen Q, Liang C, et al. HP1 links centromeric heterochromatin to centromere cohesion in mammals. *EMBO Rep*. 2018;19(4). doi:10.15252/embr.201745484
29. Yamagishi Y, Sakuno T, Shimura M, et al. Heterochromatin links to centromeric protection by recruiting shugoshin. *Nature*. 2008;455 (7210):251–255. doi:10.1038/nature07217
30. Zhang H, Chen W, Fu X, et al. CBX3 promotes tumor proliferation by regulating G1/S phase via p21 downregulation and associates with poor prognosis in tongue squamous cell carcinoma. *Gene*. 2018;654:49–56. doi:10.1016/j.gene.2018.02.043
31. Ma C, Nie XG, Wang YL, et al. CBX3 predicts an unfavorable prognosis and promotes tumorigenesis in osteosarcoma. *Mol Med Rep*. 2019;19(5):4205–4212.
32. Fan Y, Li H, Liang X, et al. CBX3 promotes colon cancer cell proliferation by CDK6 kinase-independent function during cell cycle. *Oncotarget*. 2017;8(12):19934–19946. doi:10.18632/oncotarget.15253
33. Chen LY, Cheng CS, Qu C, et al. Overexpression of CBX3 in pancreatic adenocarcinoma promotes cell cycle transition-associated tumor progression. *Int J Mol Sci*. 2018;19(6):1768.
34. Wang S, Liu F, Wang Y, et al. Integrated analysis of 34 microarray datasets reveals CBX3 as a diagnostic and prognostic biomarker in glioblastoma. *J Transl Med*. 2019;17(1):179. doi:10.1186/s12967-019-1930-3
35. Takanashi M, Oikawa K, Fujita K, et al. Heterochromatin protein 1γ epigenetically regulates cell differentiation and exhibits potential as a therapeutic target for various types of cancers. *Am J Pathol*. 2009;174(1):309–316. doi:10.2353/ajpath.2009.080148
36. Kang Y-K, Satoh T, Ryu M-H, et al. Nivolumab (ONO-4538/BMS-936558) as salvage treatment after second or later-line chemotherapy for advanced gastric or gastro-esophageal junction cancer (AGC): a double-blinded, randomized, Phase III trial. *Am Soc Clin Oncol*. 2017.
37. Zitvogel L, Galluzzi L, Kepp O, et al. Type I interferons in anticancer immunity. *Nat Rev Immunol*. 2015;15(7):405–414. doi:10.1038/nri3845
38. Sun M, Ha N, Pham DH, et al. Cbx3/HP1gamma deficiency confers enhanced tumor-killing capacity on CD8(+) T cells. *Sci Rep*. 2017;7:42888. doi:10.1038/srep42888
39. Le DT, Uram JN, Wang H, et al. PD-1 blockade in tumors with mismatch-repair deficiency. *N Engl J Med*. 2015;372 (26):2509–2520. doi:10.1056/NEJMoa1500596
40. Rizvi Naiyer A, Hellmann MD, Snyder A, et al. Mutational landscape determines sensitivity to PD-1 blockade in non–small cell lung cancer. *Science*. 2015;348(6230):124–128. doi:10.1126/science.aaa1348
41. Yarchoan M, Hopkins A, Jaffee EM. Tumor mutational burden and response rate to PD-1 inhibition. *N Engl J Med*. 2017;377 (25):2500–2501. doi:10.1056/NEJMc1713444
42. Spitzer MH, Carmi Y, Reticker-Flynn NE, et al. Systemic immunity is required for effective cancer immunotherapy. *Cell*. 2017;168 (3):487–502 e15. doi:10.1016/j.cell.2016.12.022
43. Yearley JH, Gibson C, Yu N, et al. PD-L2 expression in human tumors: relevance to Anti-PD-1 therapy in cancer. *Clin Cancer Res*. 2017;23(12):3158–3167. doi:10.1158/1078-0432.CCR-16-1761
44. Larkin J, Chiarion-Sileni V, Gonzalez R, et al. Combined nivolumab and ipilimumab or monotherapy in untreated melanoma. *N Engl J Med*. 2015;373(1):23–34. doi:10.1056/NEJMoa1504030
45. Soo LJ, Won HS, Sun DS, et al. Prognostic role of tumor-infiltrating lymphocytes in gastric cancer. *Medicine*. 2018;97(32).
46. Kim H, Choi JD, Kim B-G, et al. Interactome analysis reveals that heterochromatin protein 1γ (HP1γ) is associated with the DNA damage response pathway. *Cancer Res Treat*. 2016;48(1):322–333. doi:10.4143/crt.2014.294
47. Bilgic F, Gerceker E, Boyacioglu SO, et al. Potential role of chromatin remodeling factor genes in atrophic gastritis/gastric cancer risk. *Turk J Gastroenterol*. 2018;29(4):427–435. doi:10.5152/tjg.2018.17350
48. Guo Y, Nie Q, MacLean AL, et al. Multiscale modeling of inflammation-induced tumorigenesis reveals competing oncogenic and oncoprotective roles for inflammation. *Cancer Res*. 2017;77 (22):6429–6441. doi:10.1158/0008-5472.CAN-17-1662